

Copyright WILEY-VCH Verlag GmbH & Co. KGaA, 69469 Weinheim, Germany, 2013.

NANO MICRO
small

Supporting Information

for *Small*, DOI: 10.1002/smll.201302406

**Bioinspired Catechol-Terminated Self-Assembled Monolayers
with Enhanced Adhesion Properties**

*Mireia Guardingo, Elena Bellido, Rosa Miralles-Llumà, Jordi
Faraudo, Josep Sedó, Sergio Tatay, Albert Verdaguer, Felix
Busqué, and Daniel Ruiz-Molina**

Supporting Information for manuscript:

sml.201302406

*Bioinspired catechol-terminated self-assembled monolayers with enhanced
adhesion properties*

By Guardingo et col.

1. Monolayer characterization: PM-IRRAS

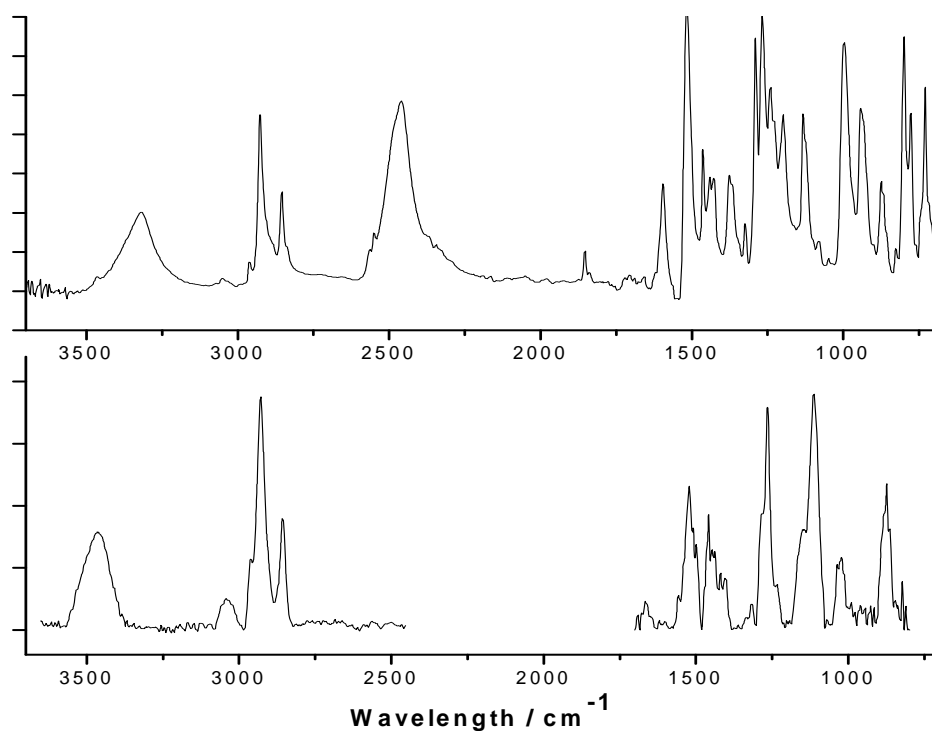


Figure S1. ATR spectra of compound **1** (above). PM-IRRAS spectra of a polycrystalline gold surface modified with a monolayer of compound **1** (below).

Band assignment	Peak position/ cm^{-1}
ν (O-H)	3462
ν (C-H)	2960, 2929, 2855
ν (C=C) _{ip}	1522, 1458
δ (O-H) _{ip} / ν (C-O)	1264
ν (C-O) / δ (O-H) _{ip}	1113
ν (C=O)	1665

Table 1. Assignment of the PM-IRRAS significant bands recorded for a SAM of **1** on polycrystalline gold (300 nm). Key: ν , stretching; δ , bending; ip, in-plane.

2. Monolayer characterization: XPS

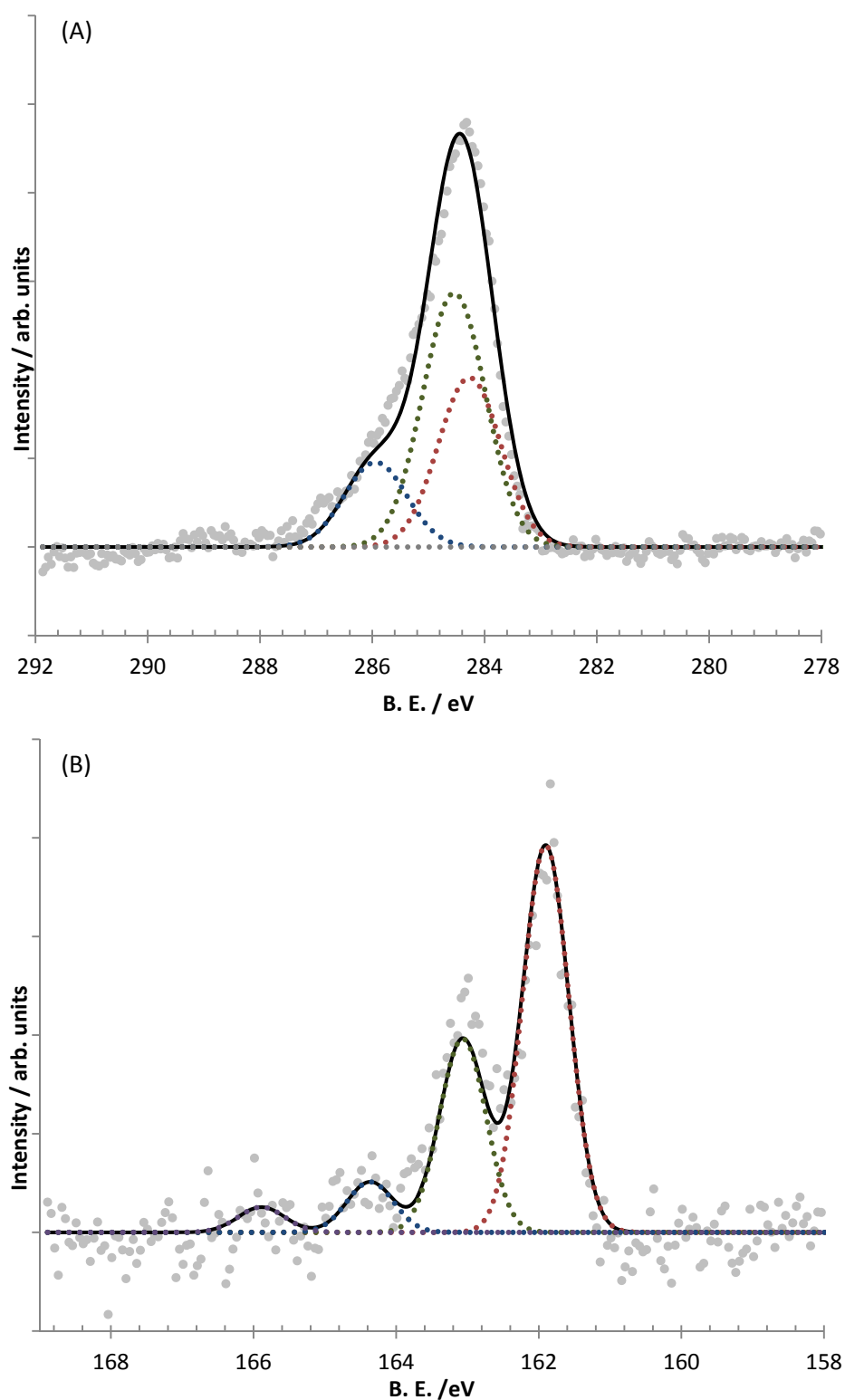


Figure S2. XPS spectra of a monolayer of compound **1** on Au. (A) C 1s core level. (B) S 2p core level.

3. Adhesion measurements: F-d curves

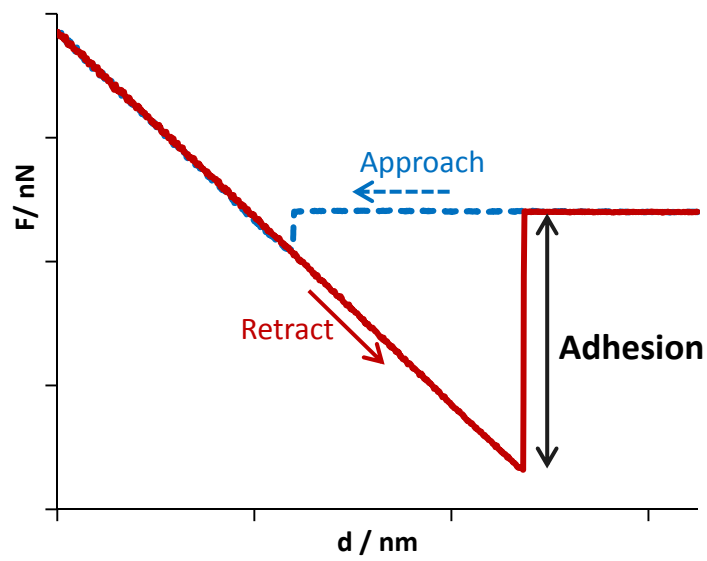


Figure S3. Model F-d curve obtained during the reported experiments. The jump-out of the tip is directly related to the adhesion force.

4. Surface topography

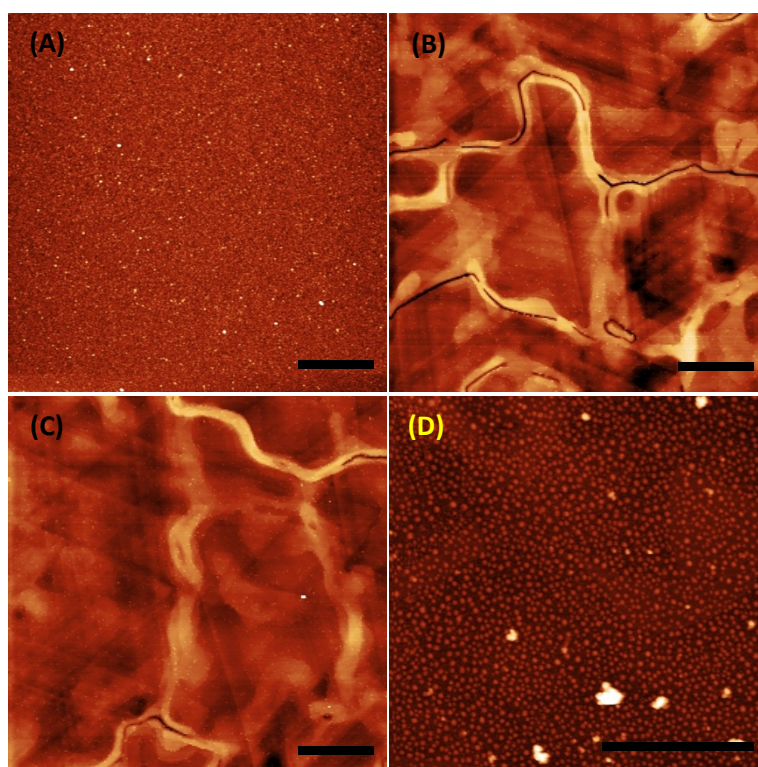


Figure S4: Tapping mode AFM topography images of the different gold substrates used in this work. (A) Polycrystalline gold (Au (40 nm)/Ti (10 nm)/Si) shows a rough topography consisting on small grains (RMS \sim 1 nm). (B) Epitaxial gold on mica (Au (300 nm)/ mica) has a smoother topography showing atomically flat terraces (RMS \sim 0.3 nm). (C) Epitaxial gold substrate that has been immersed in an ethanolic solution of compound **1**, no changes are observed in the substrate topography. (D) Epitaxial gold on mica substrate that has been coated with PDA, as shown the coating has a rough topography consisting in small aggregates which causes the loss of the substrate's smoothness and homogeneity. Scale bars are 2 μ m.

5. Magnetic nanoparticle adhesion:

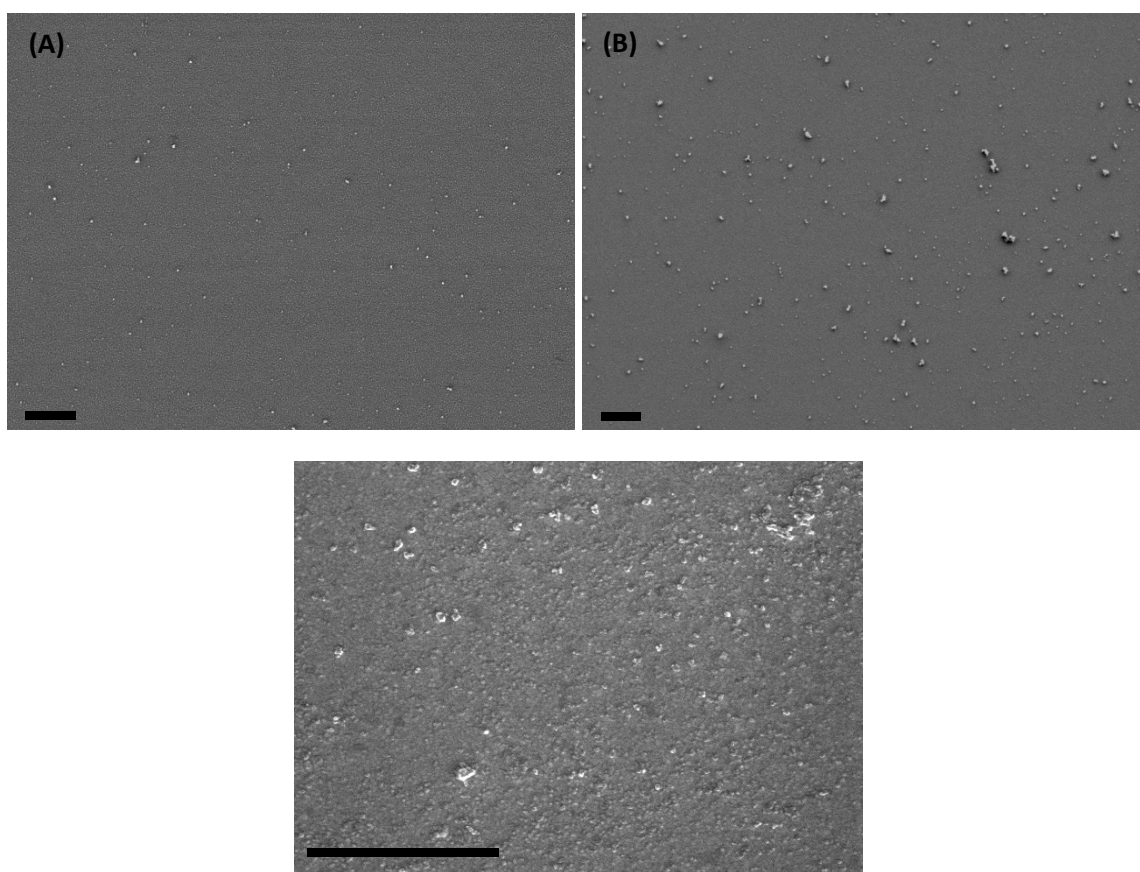


Figure S5. SEM images of PDA coated epitaxial gold substrates. (A) P-DOPA coated substrate sonicated in Milli-Q water for 15 minutes showing small aggregates of polymer on the surface. (B) PDA coated sample sonicated in a dispersion of magnetic nanoparticles (8-10 nm) for 15 minutes and then rinsed with Milli-Q water. The image denotes a poor coverage of nanoparticles. As the images show, there is not an important difference between the two samples. Small aggregates of PDA can be observed in the first sample, meaning that a portion of the aggregates observed in the second don't correspond to magnetic nanoparticles and thus, the coverage is even lower. Overall the P-DOPA coating does not act as an effective adhesive for the magnetic nanoparticles used. (C) Epitaxial gold substrate functionalised with **1** (immersion for only 15 minutes) and then sonicated in a dispersion of magnetic nanoparticles (8-10 nm) for 30 minutes and rinsed with Milli-Q water. A low and inhomogeneous coverage of nanoparticles can be observed denoting a low-density and poorly packed monolayer. Scale bars are 1 μm .

6. Adhesion measurements on early-stage monolayers.

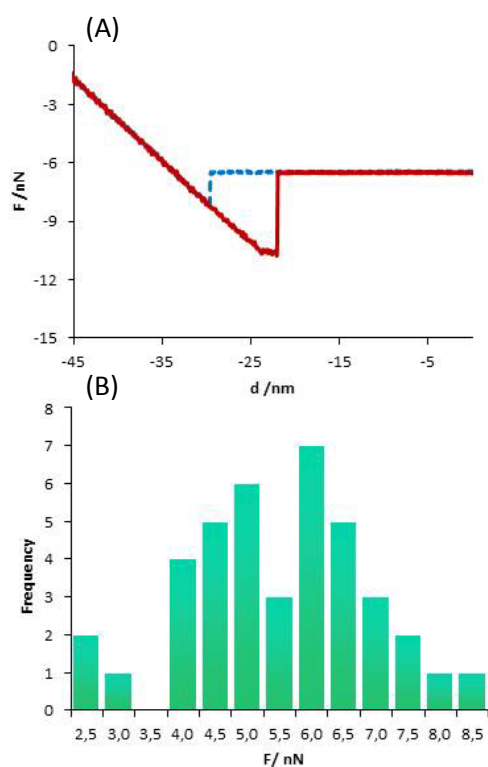


Figure S6. F-d curves obtained for an epitaxial gold substrate immersed in a solution of **1** for 15 minutes. (A) A representative force-distance curve. (B) Histogram of the measured adhesion values centred at around 5-6 nN.

7. Synthesis

3,4-bis(benzyloxy)phenyl]methanol: To a stirred solution of 3,4-bis(benzyloxy)-benzaldehyde (5.03 g, 15.8 mmol) in MeOH (72 mL) at 0 °C, sodium borohydride (1.6 g, 42.3 mmol) was added in small portions and the reaction mixture was stirred for 4 h, allowing it to warm to room temperature. At this time, the reaction was quenched by the addition of saturated NaHCO₃ solution (30 mL diluted with 30 mL of water), and extracted with CHCl₃ (4 x 30 mL). The combined organic extracts were dried (MgSO₄), filtered and concentrated under reduced pressure to furnish target alcohol (4.9 g, 15.3 mmol, 97% yield) as a white solid. The ¹H- and ¹³C-NMR spectra of the product were in good agreement with previously reported data.^[1]

1,2-bis(benzyloxy)-4-(bromomethyl)benzene (2): To a solution of [3,4-bis(benzyloxy)phenyl]-methanol (4.35 g, 13.6 mmol) in anhydrous CH₂Cl₂ (85 mL) at 0 °C, phosphorus tribromide (2.7 mL, 28.7 mmol) was added dropwise under nitrogen atmosphere. The mixture was allowed to warm to room temperature and stirred for 3 h. Then, it was quenched by the addition of water (65 mL), and the aqueous phase was extracted with CHCl₃ (3 x 63 mL). The combined organic extracts were washed with brine (2 x 40 mL), dried (MgSO₄), filtered and concentrated under reduced pressure to provide **2** (4.57 g, 11.9 mmol, 90% yield) as a pale brown solid. The ¹H- and ¹³C-NMR spectra of the product were in good agreement with previously reported data.^[1]

HRMS (ESI⁺): *m/z* calcd. for C₂₁H₁₉BrO₂Na: 405.0461 [M+Na]⁺; found, 405.0460.

[3,4-bis(benzyloxy)benzyl](triphenyl)phosphonium bromide (3): A solution of **2** (3.06 g, 7.98 mmol) and triphenylphosphine (2.77 g, 10.6 mmol) in anhydrous CH₂Cl₂ (30 mL) was refluxed under nitrogen atmosphere for 4 h. After allowing the reaction mixture to cool to room temperature, the solvent was removed under reduced pressure. The resulting solid was washed with diethyl ether, filtered and dried to afford **3** (4.99 g, 7.73 mmol, 97% yield) as a

white solid.

^1H NMR (250 MHz, CDCl_3): δ 7.64 (m, 15H), 7.31 (m, 10H), 6.89 (s, 1H), 6.65 (d, $J=8.5$ Hz, 1H), 6.59 (d, $J=8.5$ Hz, 1H), 5.34 (s, 1H), 5.29 (s, 1H), 5.04 (s, 2H), 4.78 (s, 2H); ^{13}C NMR (90 MHz, CDCl_3) δ 148.8, 148.8, 148.7, 148.6, 136.9, 136.8, 134.9, 134.9, 134.4, 134.3, 130.2, 128.4, 128.4, 128.3, 127.8, 127.7, 127.4, 127.3, 127.3, 124.6, 124.5, 119.9, 119.8, 118.3, 117.5, 117.5, 117.3, 115.0, 114.9, 71.0, 70.7, 30.5, 30.0; HRMS (ESI, m/z): $[\text{M} + \text{H}]^+$ calcd for $\text{C}_{39}\text{H}_{34}\text{O}_2\text{P}$ 565.2291 (M) $^+$, found 565.2287; Mp 198-203 $^\circ\text{C}$

5-bromopentanal: To a suspension of PCC (504 mg, 2.34 mmol) in anhydrous CH_2Cl_2 (15 mL) was added a solution of 5-bromo-1-pentanol (0.22 mL, 1.82 mmol) in anhydrous CH_2Cl_2 (5 mL) under nitrogen atmosphere. The mixture was stirred at room temperature for three hours and then 20 mL of Et_2O were added to the mixture and stirred for 10 min. The organic fraction was separated and the precipitate washed with Et_2O . The combined organic fractions were evaporated under reduced pressure to reduce to the half their volume and then filtered over a Celite pad. After evaporation of the solvents 5-bromopentanal (262 mg, 1.58 mmol, 87% yield) was obtained as a pale yellow oil. The ^1H - and ^{13}C -NMR spectra of the product were in good agreement with previously reported data.^[iii]

Z- and E-1,2-bis-(benzyloxy)-4-(6-bromo-1-hexenyl)benzene (4): To a suspension of K_2CO_3 (1.76 g, 12.77 mmol) in dry CH_2Cl_2 (15 mL) was added a small amount of 18-crown-6-ether and **3** (1.76 g, 77 mmol) under nitrogen atmosphere. To the resulting mixture was added a solution of aldehyde **4** (362.2 mg, 2.19 mmol) in dry CH_2Cl_2 (5 mL) and the mixture was refluxed under nitrogen for 24 hours. After that time, the solvent was evaporated and the crude was purified by flash column chromatography (hexane/ EtOAc 97:3) to provide a mixture 1:1 of *Z*- and *E*-**5** (496 mg, 1.09 mmol, 50% yield) as a colorless oil.

Z-4: ^1H NMR (400 MHz, CDCl_3): δ 7.46 (m, 4H), 7.40 – 7.28 (m, 6H), 6.91 (d, $J = 8.3$

Hz, 1H), 6.86 (d, $J = 1.8$ Hz, 1H), 6.79 (dd, $J = 8.3, 1.9$ Hz, 1H), 6.31 (d, $J = 11.6$ Hz, 1H), 5.51 (dt, $J = 11.6, 7.2$ Hz, 1H), 5.18 (s, 4H), 3.36 (t, $J = 6.8$ Hz, 2H), 2.22 (qd, $J = 7.3, 1.7$ Hz, 2H), 1.89 – 1.78 (m, 2H), 1.58 – 1.49 (m, 2H); ^{13}C NMR (101 MHz, CDCl_3): δ 148.65, 148.03, 137.57, 137.51, 131.43, 131.05, 129.14, 128.63, 127.93, 127.91, 127.46, 127.36, 122.35, 116.22, 115.02, 71.58, 71.55, 33.74, 32.45, 28.51, 27.66; IR (ATR): ν (cm^{-1}) = 3040, 2929, 2853, 1741, 1591, 1022; HRMS (ESI+): m/z calcd for $\text{C}_{26}\text{H}_{27}\text{BrO}_2\text{Na}$, 475.1068 $[\text{M}+\text{Na}]^+$; found: 475.1066.

E-4: ^1H NMR (400 MHz, CDCl_3): δ 7.49 – 7.41 (m, 4H), 7.40 – 7.29 (m, 6H), 6.99 (d, $J = 1.5$ Hz, 1H), 6.88 (d, $J = 8.3$ Hz, 1H), 6.85 (dd, $J = 8.3, 1.7$ Hz, 1H), 6.29 (d, $J = 15.8$ Hz, 1H), 6.01 (dt, $J = 15.7, 6.9$ Hz, 1H), 5.16 (s, 2H), 5.14 (s, 2H), 3.43 (t, $J = 6.8$ Hz, 2H), 2.22 (qd, $J = 7.3, 1.2$ Hz, 2H), 1.96 – 1.87 (m, 2H), 1.65-1.56 (m, 2H); ^{13}C NMR (101 MHz, CDCl_3): δ 149.27, 148.46, 137.42, 131.75, 129.99, 128.47, 128.44, 127.79, 127.75, 127.41, 127.34, 119.66, 115.49, 112.96, 71.59, 71.57, 33.59, 32.25, 31.99, 27.93.; IR (ATR): ν (cm^{-1}) = 3031, 2925, 2857, 1735, 1601, 1023; HRMS (ESI+): m/z calcd for $\text{C}_{26}\text{H}_{27}\text{BrO}_2\text{Na}$, 475.1068 $[\text{M}+\text{Na}]^+$; found: 475.1071.

4-(6'-bromohexyl)catechol: To a solution of a 1:1 mixture of **Z-** and **E-4** (436 mg, 0.965 mmol) in EtAcO, were added 10% Pd/C (235 mg) and acetic acid (8 μL). The mixture was stirred at room temperature under hydrogen atmosphere (3 atm) for 24 hours. Then, the suspension was filtered over a Celite® pad and the filtrate was evaporated to dryness to obtain **5** (227.8mg, 0.832 mmol, 86% yield) as a white solid.

^1H NMR (360 MHz, CDCl_3): δ 6.77 (d, $J = 8.0$ Hz, 1H), 6.70 (d, $J = 1.9$ Hz, 1H), 6.61 (dd, $J = 8.0, 1.9$ Hz, 1H), 5.47 (bs, 2H), 3.40 (t, $J = 6.8$ Hz, 2H), 2.52 (t, $J = 7.4$ Hz, 2H), 1.92 – 1.78 (m, 2H), 1.66 – 1.50 (m, 2H), 1.50 – 1.24 (m, 4H); ^{13}C NMR (63 MHz, CDCl_3): δ 143.5, 141.4, 136.0, 120.9, 115.7, 115.4, 35.1, 34.12, 32.85, 31.40, 28.4, 28.1; IR (ATR): ν (cm^{-1}) =

3328, 2930, 2856, 1606, 1110, 1059; Mp 45-49 °C (from MeOH); HRMS (ESI-): m/z calcd for $C_{12}H_{17}O_2Br$: 271.0339 $[M-H]^+$; found, 271.0345.

4-(7'-thioacetyl)hexylcatechol: To a solution of 4-(6'-bromohexyl)catechol (258 mg, 0.945 mmol) in anhydrous DMF (10 mL) were added 4Å molecular sieves and KSAc (195 mg, 1.707 mmol) under nitrogen atmosphere and the mixture was stirred at room temperature for six hours. Then, 15 mL of water were added and the aqueous phase was extracted with EtAcO (3x10 mL). The combined organic extracts were washed with water, dried ($MgSO_4$) and filtered. The crude obtained after evaporation of the solvent was purified by flash column chromatography (hexane/ EtAcO 4:1) to furnish 4-(7'-thioacetyl)hexylcatechol (210 mg, 0.782 mmol, 85% yield) as a clear oil. 1H NMR (250 MHz, $CDCl_3$): δ 6.77 (d, $J = 8.0$ Hz, 1H), 6.70 (d, $J = 1.6$ Hz, 1H), 6.58 (dd, $J = 7.9, 1.5$ Hz, 1H), 2.85 (t, $J = 7.3$ Hz, 2H), 2.48 (t, $J = 7.5$ Hz, 2H), 2.33 (s, 3H), 1.65 – 1.28 (m, 8H); ^{13}C NMR (63 MHz, $CDCl_3$): δ 197.3, 143.6, 141.6, 135.8, 120.8, 115.5, 115.3, 35.1, 31.3, 30.8, 29.4, 29.3, 28.6, 28.6; IR (ATR): ν (cm⁻¹) = 3370, 2928, 2855, 1664, 1606; HRMS (ESI-): m/z calcd for $C_{14}H_{20}O_3S$ $[M-H]^+$: 267.1060; found: 267.1051.

4-(6'-mercaptohexyl)catechol (1): 4-(7'-thioacetyl)hexylcatechol (210 mg, 0.782 mmol) was dissolved in a degassed 1:1 mixture of 0.2 M NaOH and EtOH (14 mL) and the resulting solution was stirred under argon at room temperature for three hours. At this time, the mixture was extracted with EtAcO (3x10 mL) and the combined organic fractions were dried ($MgSO_4$), filtered and evaporated to dryness. The crude was purified by flash column chromatography (hexane/EtAcO 2:1) to provide **1** (86 mg, 0.38 mmol, 49% yield) as well as the corresponding disulfide (23 mg, 0.051 mmol, 13% yield).

Thiol **1**: 1H NMR (250 MHz, MeOD): δ 6.65 (d, $J = 8.0$ Hz, 1H), 6.59 (d, $J = 2.0$ Hz, 1H), 6.47 (dd, $J = 8.0, 2.0$ Hz, 1H), 2.46 (td, $J = 7.3, 5.4$ Hz, 4H), 1.65 – 1.48 (m, 4H), 1.48 – 1.23 (m, 4H); ^{13}C NMR (101 MHz, MeOD): δ 145.85, 143.90, 135.55, 120.59, 116.44, 116.12,

36.09, 35.09, 32.66, 29.62, 29.18, 24.92; IR (ATR): ν (cm^{-1}) = 3318, 2925, 2854, 2459, 1517, 874; Mp 58-61 °C; HRMS (ESI-): m/z calcd for $\text{C}_{12}\text{H}_{18}\text{O}_2\text{S}$: 225.0955 [M-H^+]; found: 225.0949.

Disulfide: ^1H NMR (250 MHz, CDCl_3): δ 6.65 (d, $J = 8.0$ Hz, 1H), 6.60 (d, $J = 2.0$ Hz, 1H), 6.47 (dd, $J = 8.0, 2.0$ Hz, 1H), 2.66 (t, $J = 7.2$ Hz, 2H), 2.45 (t, $J = 7.5$ Hz, 2H), 1.73 – 1.48 (m, 4H), 1.48 – 1.25 (m, 4H); ^{13}C NMR (63 MHz, CDCl_3): δ 146.0, 144.1, 135.6, 120.6, 116.5, 116.2, 39.7, 36.1, 32.7, 30.1, 29.8, 29.3. IR (ATR): ν (cm^{-1}) = 3255, 2920, 2850, 1603; Mp 67-71 °C; HRMS (ESI-): m/z Calcd for $\text{C}_{24}\text{H}_{34}\text{O}_4\text{S}_2\text{Na}$ [M-H^+]: 449.1826; found: 449.1820

In order to improve the overall yield, the disulfide was reduced to obtain the thiol **1**. To a solution of **7** (21 mg, 0.047 mmol) in degassed MeOH (5 mL), was added PBU_3 (15 μL , 0.061 mmol) and the mixture was stirred at room temperature under argon atmosphere for four hours. Then, the reaction was quenched by the addition of water (5 mL) and the aqueous phase was extracted with EtAcO. The combined organic fractions were dried (MgSO_4), filtered and concentrated by evaporation under reduced pressure. The crude was purified by flash column chromatography (hexane/ EtOAc 2:1) to obtain **1** (16 mg, 0.07 mmol, 74% yield) as a white solid.

8. Molecular Dynamics Simulations.

The model for the molecules was based on the CHARMM22/CMAP force field,^[iii] designed for biomolecular simulations. In our simulations here we employ standard CHARMM atom types. The modular structure of this force field (constructed from quantum chemical calculations of the interactions between model compounds) allows one to construct the model parameters for a given organic compound from the basic building blocks of the force field. Within this force field, intramolecular interactions contained bonding, torsion and dihedral potentials and intermolecular interactions were described by electrostatic interactions (modelled with partial charges) plus a Lennard-Jones interaction potential. The employed values for the interaction parameters for water (TIP3P model) are the standard values in the CHARMM22 force field. The force field for Au atoms and their interactions with organic molecules was taken from a new improved Lennard-Jones parameterization, accurate for interfacial calculations and compatible with the CHARMM force field.^[iv] The parameters employed for the catechol group were the same employed in our previous simulations of compounds containing catechol moieties.^[v] A NAMD topology file containing the values of the force field parameters required for the simulation is available from the authors upon request.

In our simulations, we have considered a gold slab of 7.2079 nm² containing a total of 300 Au atoms arranged in 3 layers of Au atoms stacked along the <111> orientation of the fcc structure. The surface was covered with different numbers of compound 1 molecules (1, 2, 4, 6, 10, 15, 19, 21, 24,26, 28). In this way, we simulate SAMs corresponding to different surface coverage, ranging from 0.14 to 3.88 molecules/nm². We have considered simulations with solvent and in vacuum conditions. In vacuum simulations, the size of the simulation box perpendicular to the gold surface was 10 nm. In the simulations with water as a solvent, this vertical size fluctuates (due to the use of a barostat) and has an equilibrium size of 8.2 nm

(between 1580 and 1785 water molecules, depending on the simulation). These quantities of solvent were large, and they provide not only solvation for the surface and SAM but also provide a bulk-like liquid far from the monolayer.

Before running the MD simulations, we have to create suitable initial configurations of the molecules and the surface involved in the simulations. First, we built the gold slab following the same procedure described in our previous work.^[v(b)] Then, the desired number of compound **1** molecules were adsorbed onto the gold surface by attaching the sulphur atom to a Au surface atom. In the simulations with solvent, we add the solvent molecules from a previously equilibrated solvent slab, employing the “solvate” tool of the VMD 1.9.1 program.^[vi] The obtained configuration was energy minimized as described in previously in order to obtain suitable initial configurations for the MD simulations.^[v(b)] In order to save computational time, in our MD simulations we considered fixed the positions of the Au atoms of the surface, as in our previous works. Also, we froze the S atoms linked to Au atoms. Therefore, in the MD simulations we solved the equations of motion for the atoms of the compound **1** molecules (except S atoms) and solvent molecules. The length of the simulation runs and the length of the equilibration and production time were determined by monitoring the time evolution of the quantities of interest in the simulation (energy and structural quantities). In particular, we monitored the evolution of the angle of all the catechol moieties with the surface normal (since this is a quantity of experimental interest) by employing a home-made python script running in VMD 1.9.1 (available from the authors upon request). We observed that these angles equilibrate after times of the order of 5-10 ns in the case of simulations with solvent and 1-2 ns in the case of simulations in absence of solvent. In order to obtain reasonable statistics, the typical length of each MD simulation run was about 10 ns in absence of solvent and about 50 ns in the case of solvent simulations (although the exact duration was different in each specific simulation, depending on the exact

duration of equilibration and the noise in the angle evaluations).

-
- [i] (a) K. A. Brun, A. Linden, H. Heimgartner, *Helvetica Chimica Acta*. **2002**, 85, 3422-3433. (b) S. Venkateswarlu, B. Satyanarayana, C. V. Sureshbabu, G. V. Subbaraju, *Biosci. Biotechnol. Biochem.* **2003**, 67, 2463-2466. (c) K. Thakkar, R. L. Geahlen, M. Cushman, *J. Med. Chem.* **1993**, 36, 2950-2955. (d) V. Percec, M. Peterca, M. Sienowska, M. A. Ilies, E. Aqad, J. Smidrkal, P. A. Heiney, *J. Am. Chem. Soc.* **2006**, 128, 3324-3334.
- [ii] M. Miesch, L. Miesch, P. Horvatovich, D. Burnouf, H. Delincee, A. Hartwig, F. Raul, D. Werner, E. Marchioni, *Radiat. Phys. Chem.*, **2002**, 65, 233-239, (b) W. R. Dolbier Jr., X. X. Rong, M. D. Bartberger, H. Korionak, B. E. Smart, Z. Yang, *J. Chem. Soc., Perkin Trans.* **2.1998**, 2, 219-231.
- [iii] a) A.D.MacKerell, et al.,*J.Phys.Chem.B* **1998**,102,3586. b) A. D. MacKerell Jr., M. Feig, C. L. Brooks III, *J. Comput. Chem.* **2004**, 25, 1400.
- [iv] H.Heinz, R.A.Vaia, B.L.Farmer, R.R.Naik, *J.Phys.Chem. C* **2008**, 112, 17281.
- [v] a) J. Saiz-Poseu, J. Faraudo, A. Figueras, R. Alibes, F. Busqué, D. Ruiz-Molina *Chem. Eur. J.* **2012**, 18, 3056. b) J. Saiz-Poseu, A. Martínez-Otero, Th. Roussel, J. K.-H. Hui, M. L. Montero, R. Urcuyo, M. J. MacLachlan, J. Faraudo, D. Ruiz-Molina, *Phys. Chem. Chem. Phys.* **2012**, 14, 11937. c) J. Saiz-Poseu, I. Alcón, R. Alibés, F. Busqué, J. Faraudo, D. Ruiz-Molina, *CrystEngComm*, **2012**, 14, 264.
- [vi] W.Humphrey, A. Dalke, K. Schulten, *J. Molec. Graphics*, **1996**, 14, 33.